EUROPEAN JOURNAL OF PURE AND APPLIED MATHEMATICS
Vol. 16, No. 2, 2023, 736-750
ISSN 1307-5543 – ejpam.com
Published by New York Business Global

A Host-parasitoid Dynamics with Allee and Refuge effects

Burcin Kulahcioglu[1], Unal Ufuktepe[2,*], Antonios Kalampakas[2]

[1] *Faculty of Engineering and Architecture, Beykoz University, Istanbul, Turkey*
[2] *College of Engineering and Technology, American University of the Middle East, Kuwait*

Abstract. We examine a discrete-time host–parasitoid model incorporating simultaneously an Allee and a refuge effect on the host. We investigate existence of a positive fixed point, local asymptotic stability, global stability of the fixed points and bifurcations. Numerical examples are given for verification of the theoretical results and we compare the model with existing data from the literature.

2020 Mathematics Subject Classifications: 92D25, 39A30, 92D30

Key Words and Phrases: Discrete dynamical systems, Host-parasitoid, Nicholson-Bailey, Bifurcation, Allee effect, Refuge effect

1. Introduction

Discrete dynamic systems (DDS) in general have been studied extensively and particularly in the recent period in view of the Coronavirus disease pandemic [16],[21],[1],[17],[22]. In addition, it has been shown that population dynamics implementing DDS can produce efficient computational results for host-parasitoid interactions with numerical simulations [18],[9],[20], see also [11]. Parasitoids are insect species whose larvae developed by feeding on the bodies of other arthropods, usually killing them. Larvae emerge from the host and developed into free-living adults. The adults then lay their eggs in a subsequent generation of hosts. The host-parasitoid dynamics are increasingly being studied for habitat management [13], controlling invasive pests [5] and [14], identifying movement among habitat patches [4] and internal Host-Parasitoid variations [19]. The general framework for the study of discrete-type host-parasitoid model is the following:

$$\begin{aligned} H_{t+1} &= rH_t f(H_t, P_t), \\ P_{t+1} &= \beta H_t \left(1 - f(H_t, P_t)\right), \end{aligned} \tag{1}$$

*Corresponding author.
DOI: https://doi.org/10.29020/nybg.ejpam.v16i2.4707

Email addresses: burcinkulahcioglu@beykoz.edu.tr (B. Kulahcioglu), unal.ufuktepe@aum.edu.kw (U. Ufuktepe), antonios.kalampakas@aum.edu.kw (A. Kalampakas)

where H_t and P_t are population sizes of host and parasitoids, respectively, in the generation t. In the host population, r is the reproduction rate of hosts, and the function $f(H_t, P_t)$ is the fraction of host escaping parasitism. In the parasitoid equation, β is the average number of eggs (larvae) released by parasitoid on a single host.

An ecologically interesting model developed to describe population dynamics of a coupled host-parasitoid system is the Nicholson–Bailey model [12] which adds further assumptions to the general case. Since most parasitoid larvae require a specific life-stage of the host, the parasitoid and host generations are lined to one another [7]. Hence the total number of encounters with hosts by parasitoids is in direct proportion to host density and the encounter number is distributed randomly among the available hosts. Using Poisson distribution model 1 becomes:

$$\begin{aligned} H_{t+1} &= rH_t e^{-aP_t} \\ P_{t+1} &= \beta H_t \left(1 - e^{-aP_t}\right), \end{aligned} \tag{2}$$

where e^{-aP_t} stands for probability of not to be infested by parasitoid and $1 - e^{-aP_t}$ is the probability of being infested by parasitoid at time t.

Initial studies on host-parasitoid interactions employed Equations (2), known as Nicholsan-Bailey host-parasitoid model. Several other host-parasitoid models have since been developed as versions of Nicholsan-Bailey (see e.g. [15]-[2]).

In [11] the 2-year oscillations in abundance of Xestia moths were investigated by testing a hypothesized Xestia-Ophion interaction. Using statistical modelling of time-series data the authors provided evidence demonstrating the validity of an underlying host-parasitoid hypothesis (see also [15]). The governing model is

$$\begin{aligned} N_{t+2} &= N_t g(N_t) f(P_t), \\ P_{t+1} &= N_t (1 - f(P_t)), \end{aligned} \tag{3}$$

where N_t and P_t are the population sizes of the host (Xestia) and parasitoid (Ophion), respectively. The function $g(N)$ denotes the population growth rate of the host and the function $f(P)$ is the fraction of hosts that are not parasitised. This model assumes a 2-year host life cycle as opposed to single year life cycle of the parasitoid which explains the apparent 2-year population oscillation. For this reason there are two independent host populations one for even and one for odd years. Although there is no direct interaction between the two host cohorts, they are coupled through the the parasitoid population. When we checked their open source data with Minitab (see Figure 12., Figure 13., and Figure 14.) there is only one fixed point which is (0,0) and the the fraction of the host escaping parasitism is periodic and piece-vise exponential because of the seasonal behavior of the parasitoid.

Unlike the predator in the general prey-predator models, the parasitoid in the host-parasitoid models has a production rate closely defined by interactions between host and parasitoid. Hence, generally it is sufficient to use a density dependent population model for the host, which is also thought to stabilize the system [2]. In [10], 3 different model

types were proposed according to the ordering of parasitism and density dependence. In this approach, when parasitism acts first and density dependence takes places only on the survivors from parasitism (i.e. $H_t f(P_t)$) the model type is:

$$\begin{aligned} H_{t+1} &= H_t g(H_t, f(P_t)) f(P_t), \\ P_{t+1} &= H_t \left(1 - f(P_t)\right). \end{aligned} \tag{4}$$

Choosing $f(P_t) = exp(-bP_t)$, $g(H_t, f(P_t)) = \lambda/(1 + kH_t exp(-bP_t))$ and adding β multiplier to the second equation, we obtain:

$$\begin{aligned} H_{t+1} &= \frac{\lambda H_t}{1 + kH_t e^{-bP_t}} e^{-bP_t}, \\ P_{t+1} &= \beta H_t (1 - e^{-bP_t}). \end{aligned} \tag{5}$$

This model (5) was formulated and analyzed in [6]. In this setup, the host population in the absence of the parasitoid is modeled by Beverton-Holt equation $\lambda H/(1 + kH)$. The parameter β represents the average number of egg (larvae) released by parasitoid on a single host and all parameters are positive. Allee and the refuge effects were separately added to this model in [8].

In this paper, we incorporate both effects simultaneously and study the dynamics of the resulting model. Our discrete-time host–parasitoid model is presented in section 2. In section 3 we determine the conditions under which a positive fixed point exists and is unique. In Section 4 we study local asymptotic stability, global fixed point stability and types of bifurcations. Numerical examples for verification of the theoretical results are given in Section 5 where the data of [11] are checked with Minitab in comparison to our model.

2. Host–parasitoid model with Allee and refuge effects

In this section we will introduce a discrete-time host–parasitoid model incorporating simultaneously an Allee and a refuge effect on the host. We start from the system of equations (5). It has four parameters, namely, λ, b, k and β. We can simplify it by substituting $N_t = \beta H_t$ and $y_t = bP_t$.

$$\begin{aligned} N_{t+1} &= \frac{\lambda N_t}{1 + \frac{k}{\beta} N_t e^{-y_t}} e^{-y_t}, \\ y_{t+1} &= bN_t \left(1 - e^{-y_t}\right). \end{aligned} \tag{6}$$

Let $x_t = bN_t$ and $c = k/(\beta b)$, then the model (6) can be written as follows:

$$\begin{aligned} x_{t+1} &= \frac{\lambda x_t e^{-y_t}}{1 + c x_t e^{-y_t}}, \\ y_{t+1} &= x_t \left(1 - e^{-y_t}\right), \end{aligned} \tag{7}$$

where x_t and y_t denotes the population sizes of host and parasitoid, respectively at time t. We add a constant proportion refuge effect and the mate limitation Allee effect to the model (7). We obtain:

$$\begin{aligned} x_{t+1} &= \frac{(1-\Psi)\lambda x_t}{1+cx_t}\frac{x_t}{s+x_t} + \frac{\Psi\lambda x_t e^{-y_t}}{1+cx_t e^{-y_t}}\frac{x_t}{s+x_t}, \\ y_{t+1} &= \Psi x_t\left(1-e^{-y_t}\right), \end{aligned} \tag{8}$$

where $0 < \Psi \leq 1$ is the proportion of host available to parasitoid, $(1-\Psi)$ is proportion of protective refuge, and $s > 0$ is the Allee effect constant. In the following sections we will study the dynamics of (8).

3. Fixed Points

In this section we find the fixed points of the system, and identify conditions for the existence and uniqueness of a positive fixed point.

$$\begin{aligned} x &= \frac{(1-\Psi)\lambda x}{1+cx}\frac{x}{s+x} + \frac{\Psi\lambda x e^{-y}}{1+cxe^{-y}}\frac{x}{s+x}, \\ y &= \Psi x\left(1-e^{-y}\right). \end{aligned} \tag{9}$$

(i) $F_0 = (0,0)$ is extinction fixed point for all values of parameters.

(ii) $F_1 = (\frac{A+\sqrt{A^2-4cs}}{2c}, 0)$ and $F_2 = (\frac{A-\sqrt{A^2-4cs}}{2c}, 0)$ are axial fixed points where $A = \lambda - cs - 1$ for $\left(1+\sqrt{cs}\right)^2 \leq \lambda$ (extinction of the parasite).

(iii) Let $F_3 = (x^*, y^*)$ (the host and the parasite survive) be the positive fixed point, where $x^* = \frac{y^*}{\Psi(1-e^{-y^*})}$ by the second equation of (9). First, we show the existence of F_3. If we substitute $x = y/(\Psi(1-e^{-y}))$ in the first equation of (9), we obtain

$$\frac{1}{\lambda} = f(y) + g(y), \tag{10}$$

where

$$f(y) = \frac{(1-\Psi)\Psi e^y\left(e^y-1\right)y}{\left(\Psi\left(e^y-1\right)s + e^y y\right)\left(e^y(\Psi+cy)-\Psi\right)}, \tag{11}$$

and

$$g(y) = \frac{\Psi^2\left(e^y-1\right)y}{\left(\Psi\left(e^y-1\right)+cy\right)\left(\Psi\left(e^y-1\right)s + e^y y\right)}. \tag{12}$$

Since

$$g'(y) = -\frac{\Psi^2 e^y y\left(e^y-y-1\right)}{\left(\Psi\left(e^y-1\right)+cy\right)\left(\Psi\left(e^y-1\right)s+e^y y\right)^2} -$$

$$\frac{\Psi^3\left(e^y-1\right)\left(1+e^y(y-1)\right)}{\left(\Psi\left(e^y-1\right)+cy\right)^2\left(\Psi\left(e^y-1\right)s+e^y y\right)}<0, \quad (13)$$

the function $g(y)$ is a decreasing function of y.

And we have

$$\lim_{y\to 0} g(y)=\frac{\Psi^2}{(c+\Psi)(1+\Psi s)} \quad (14)$$

Now, we continue with the graphical properties of $f(y)$.

$$f'(y)=\frac{(1-\Psi)\Psi e^y\left(e^y-y-1\right)\left(\Psi^2\left(e^y-1\right)^2 s-ce^{2y}y^2\right)}{\left(\Psi\left(e^y-1\right)s+e^y y\right)^2\left(\Psi-e^y(\Psi+cy)\right)^2}. \quad (15)$$

If $s<\frac{c}{\Psi^2}$, then $f'(y)<0$, which means $f(y)$ is decreasing function. And also

$$\lim_{y\to 0} f(y)=\frac{(1-\Psi)\Psi}{(c+\Psi)(1+\Psi s)}. \quad (16)$$

Let $h(y)=f(y)+g(y)$, $h(y)$ is a decreasing function of y if $s<\frac{c}{\Psi^2}$. And

$$\lim_{y\to 0} h(y)=\frac{(1-\Psi)\Psi}{(c+\Psi)(1+\Psi s)}+\frac{\Psi^2}{(c+\Psi)(1+\Psi s)}=\frac{\Psi}{(c+\Psi)(1+\Psi s)} \quad (17)$$

The positive fixed point exists if $\lambda=\frac{1}{h(y)}$ where $h(y)\neq 0$. $\frac{1}{h(y)}$ is an increasing function of y and

$$\lim_{y\to 0}\frac{1}{h(y)}=\frac{(c+\Psi)(1+\Psi s)}{\Psi}. \quad (18)$$

As a result (See Figure 1) a positive fixed point exists and it is unique if $s<\frac{c}{\Psi^2}$ and $\lambda>\frac{(c+\Psi)(1+\Psi s)}{\Psi}$. Otherwise, neither the existence nor the uniqueness is guaranteed (Figure 2 and Figure 3).

4. Local Asymptotic Stability and Global Behaviors

In this section we investigate local asymptotic stability, global stability and bifurcations. The corresponding Jacobian matrix of (8) is as follows:

$$J_A=\begin{pmatrix} \frac{\lambda x\left((e^y+cx)^2(x+s(2+cx))-\Psi(-1+e^y)\left(e^y(2s+x+csx)+cx\left(s-cx^2\right)\right)\right)}{(s+x)^2(1+cx)^2\left(e^y+cx\right)^2} & -\frac{\lambda\Psi e^y x^2}{(s+x)\left(e^y+cx\right)^2} \\ \Psi\left(1-e^{-y}\right) & \Psi e^{-y}x \end{pmatrix}.$$

(i) $J_A(F_0)$ is 0 matrix, so F_0 is stable for all parameter values by Trace-determinant Theorem (see Figure 4. , and Figure 9.).

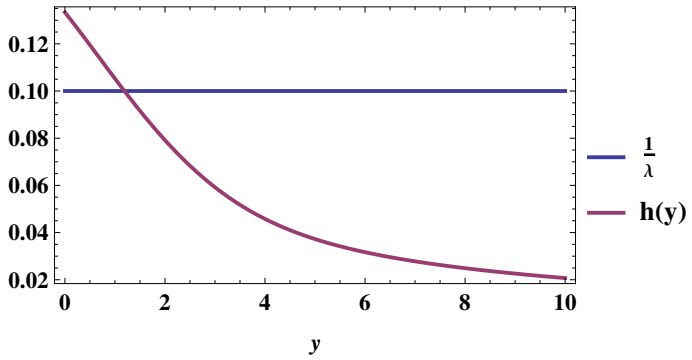

Figure 1: The positive fixed point of the model (8) exists if the two functions intersect. If $s < \frac{c}{\Psi^2}$ and $\lambda > \frac{(c+\Psi)(1+\Psi s)}{\Psi}$, they intersect once (unique positive fixed point). The figure depicts this case for $\lambda = 10$, $c = 1$, $s = 3$, and $\Psi = 0.5$.

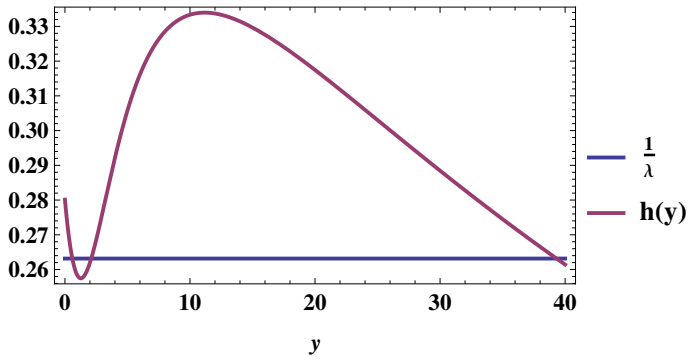

Figure 2: The case $s > \frac{c}{\Psi^2}$ for $\lambda = 3.8$, $c = 0.01$, $s = 5$, and $\Psi = 0.5$.Multiple intersections, multiple positive fixed points.

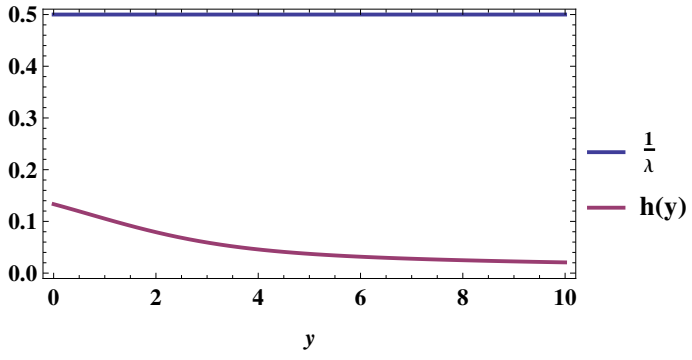

Figure 3: The case $\lambda < \frac{(c+\Psi)(1+\Psi s)}{\Psi}$ for $\lambda = 2$, $c = 1$, $s = 3$, and $\Psi = 0.5$. The positive fixed point of the model (8) exists if the two functions intersect.No intersection, no positive fixed point.

(ii) The Jacobian matrix evaluated at F_1 is

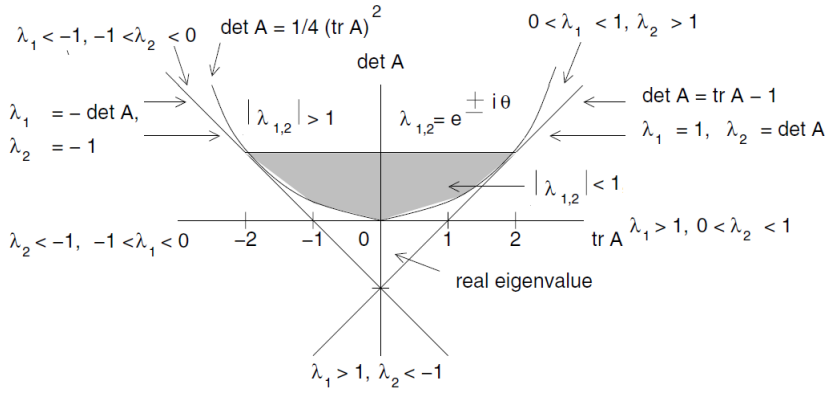

Figure 4: The determinations of eigenvalues in all the regions in the Det-Trace plane [3].

$$J_A(F_1) = \begin{pmatrix} 1 - \frac{\sqrt{A^2-4cs}}{\lambda} & \frac{\Psi\left(1-\lambda-cs-\sqrt{A^2-4cs}\right)}{2\lambda c} \\ 0 & \frac{\Psi\left(A+\sqrt{A^2-4cs}\right)}{2c} \end{pmatrix}.$$

We have $\lambda_1 = 1 - \frac{\sqrt{A^2-4cs}}{\lambda}$ and $\lambda_2 = \frac{\Psi\left(A+\sqrt{A^2-4cs}\right)}{2c}$. Hence, $|\lambda_{1,2}| < 1$ if $s < \frac{c}{\Psi^2}$ and $(1+\sqrt{cs})^2 < \lambda < \frac{(c+\Psi)(1+\Psi s)}{\Psi}$. Under these conditions F_1 is stable (see Figure 4. , and Figure 11.).

(iii) The Jacobian matrix at F_2 is

$$J_A(F_2) = \begin{pmatrix} 1 + \frac{\sqrt{A^2-4cs}}{\lambda} & \frac{\Psi\left(1-\lambda-cs+\sqrt{A^2-4cs}\right)}{2\lambda c} \\ 0 & \frac{\Psi\left(A-\sqrt{A^2-4cs}\right)}{2c} \end{pmatrix}.$$

We have $\lambda_1 = 1 + \frac{\sqrt{A^2-4cs}}{\lambda}$ and $\lambda_2 = \frac{\Psi\left(A-\sqrt{A^2-4cs}=det()\right)}{2c}$.

Case 1: If $A^2 = 4cs \Rightarrow \lambda_1 = 1$ and $\lambda_2 = \frac{\Psi A}{2c} = det(J_A)$ so we have non-hyperbolic case and it is saddle-node (Fold) Bifurcation if $0 < \lambda_2 < 1$ then by the Center Manifold theory[3] F_2 is oscillatory: It is oscillatory source If $\Psi A > 2c$. It is oscillatory saddle if $\Psi A < 2c$.

Case 2: If $A^2 - 4cs > 0$ then $\lambda_1 > 1$ and F_2 is a spiral source. (see Figure 5. ,Figure 6, and Figure 10.)

Numerical simulations to investigate the behavior of the fixed point F_3 will be implemented in Section 5.

For the model (8), $F_0 = (0, 0)$ is globally asymptotically stable if $\lambda < 1$. We have

$$x_{t+1} = \frac{(1-\Psi)\lambda x_t}{1+cx_t}\frac{x_t}{s+x_t} + \frac{\Psi\lambda x_t}{e^{y_t}+cx_t}\frac{x_t}{s+x_t}$$

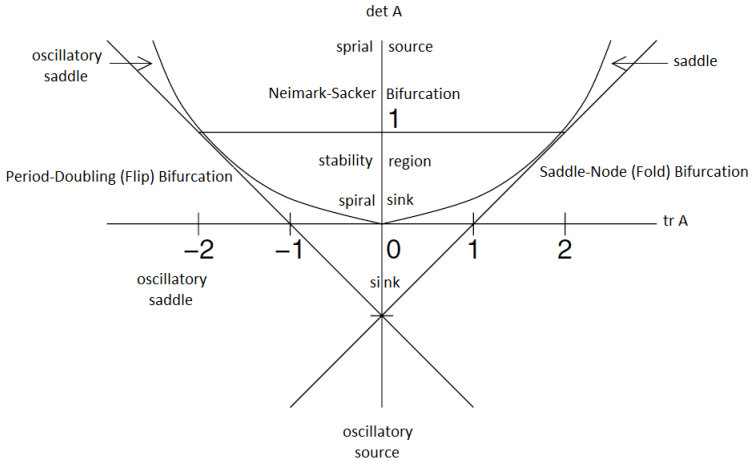

Figure 5: Classification of the fixed points and bifurcations in all the regions in the Det-Trace plane.

By comparison we obtain

$$x_{t+1} \leq \frac{\lambda x_t}{1+cx_t}\frac{x_t}{s+x_t} < \frac{\lambda x_t}{1+cx_t} < \lambda x_t < x_t$$

if $\lambda < 1$. Then

$$\lim_{t\to\infty} x_t = 0,$$

which also implies

$$\lim_{t\to\infty} y_t = 0.$$

Hence, the fixed point F_0 is globally attracting if $\lambda < 1$, and it is locally asymptotically stable for all values of parameters. Thus, it is globally asymptotically stable if $\lambda < 1$.

The global behavior of the other fixed points is omitted, since local stability of $(0,0)$ does not allow any other fixed points to behave stable, globally. Since F_0 is locally asymptotically stable for all values of parameters, at least with a very small initial value, the system goes to extinction even with a large growth parameter λ. As a result, the other points cannot be globally attractive.

5. Numerical Simulations

In this section we verify the theoretical results of our model by numerical simulations and compare it by using the data of [11] by using Minitab. In order to investigate the impact of λ to the model, we fix $c = 1$, $\Psi = 0.5$, and $s = 0.5$ and consider cases, which satisfy the conditions $s < \frac{c}{\Psi^2}$ and $\lambda > \frac{(c+\Psi)(1+\Psi s)}{\Psi}$.

Assume that $\lambda = 4$. Then the positive fixed point is $F_3 = (2.16476, 0.160471)$ with corresponding eigenvalues $(0.834265, 0.608611)$. As a result, F_3 is a sink. In Figure 6, we

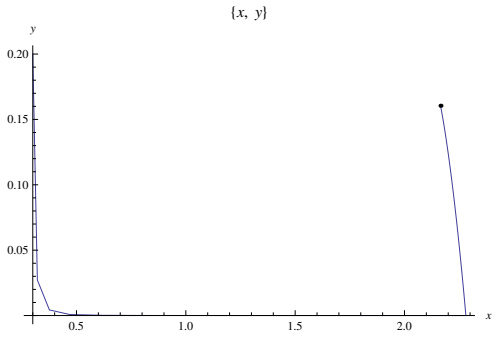

Figure 6: Phase portrait for the model (8) for $\Psi = 0.5$, $c = 1$, $s = 0.5$ and $\lambda = 4$.

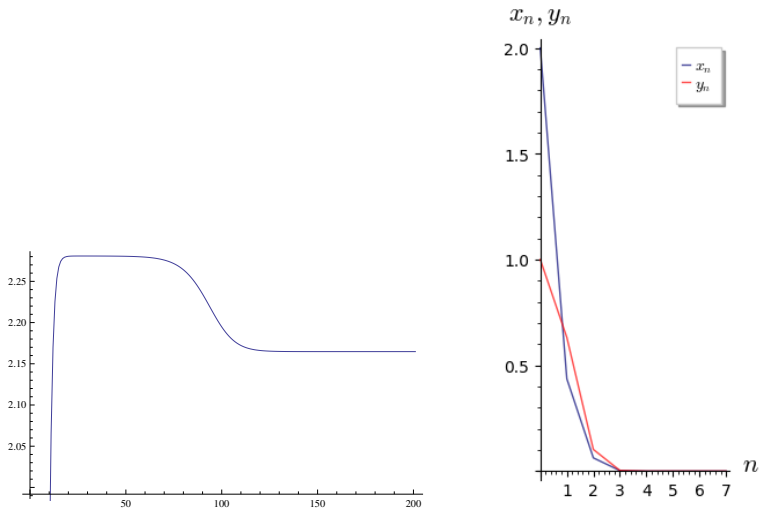

Figure 7: a) Time series of x for the model (8) for $\Psi = 0.5$, $c = 1$, $s = 0.5$ and $\lambda = 4$. b) Time series of (x, y) for the model (8) for $\lambda = 2$, $s = 3$, $c = 1$, $\Psi = 0.5$.

give the phase portrait and we give the times series diagrams in Figure 7. If we assign a large growth rate $\lambda = 10$, then the fixed point $F_3 = (5.31214, 2.41985)$ and eigenvalues are $0.312199 \pm 0.669214i$. F_3 is a spiral sink. We observe that the positive fixed point remains stable for a large interval of growth parameter λ. In Figure 8, we give the bifurcation diagram.

Finally, we give the basin of attraction for the model (8) in Figures 9-11. In the analytical results, we show that the fixed point $F_0 = (0, 0)$ is stable for all values of parameters. In the numerical simulations, we show that the positive fixed point F_3 is stable for $\Psi = 0.5$, $c = 1$, $s = 0.5$ and $\lambda = 4$. We present the basin of attraction to show the set of points which are eventually iterated to either F_0 or F_3 under this set of parameters. On the other hand, if we let $s = 0$, that means there is no Allee Effect. By keeping the other parameters the same, only the positive fixed point is stable. For the basin of attraction code, we refer to [18].

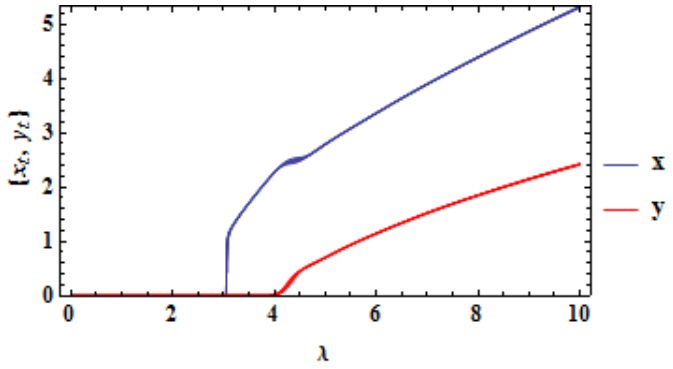

Figure 8: The bifurcation diagram of the model (8) for $s = 0.5$.

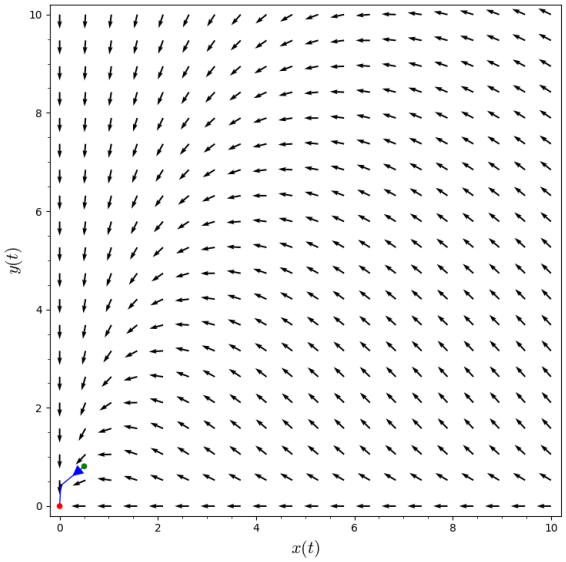

Figure 9: Initial point (2,1) $\lambda = 2$, $s = 3$, $c = 1$, $\Psi = 0.5$.

6. Conclusion

In this paper, the complex dynamics of a nonlinear discrete-time host-parasitoid system with Allee and refuge effects are analyzed. We examined fixed point stability and bifurcations and investigated global and local fixed point stability. By the study of numerical simulations with the data of [11] using Minitab and our Mathematica codes we find that the behavior of the system is simultaneously periodic and chaotic. A future research direction is to create a specific model for this type of data with hybrid models.

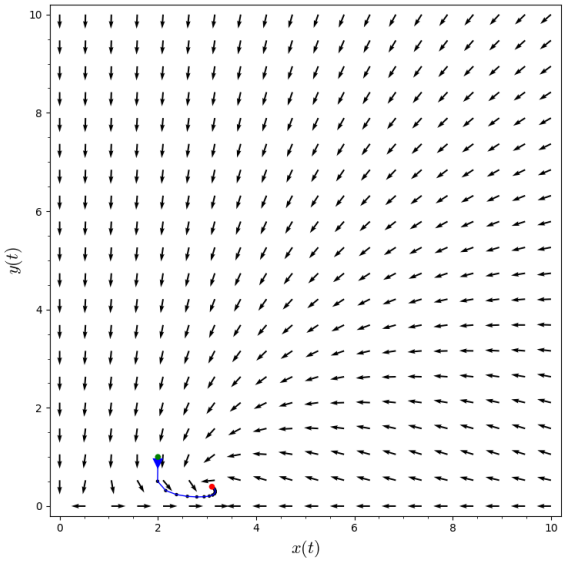

Figure 10: Initial point (2,1) $\lambda = 7$, $s = 2$, $c = 1$, $\Psi = 0.4$.

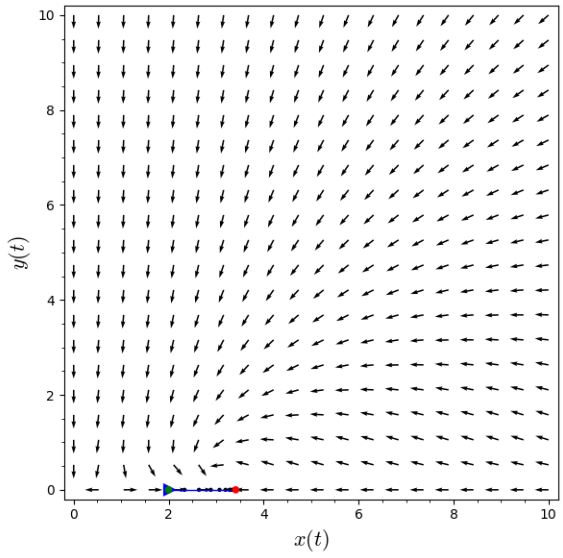

Figure 11: Initial point (2,0) $\lambda = 7$, $s = 2$, $c = 1$, $\Psi = 0.4$

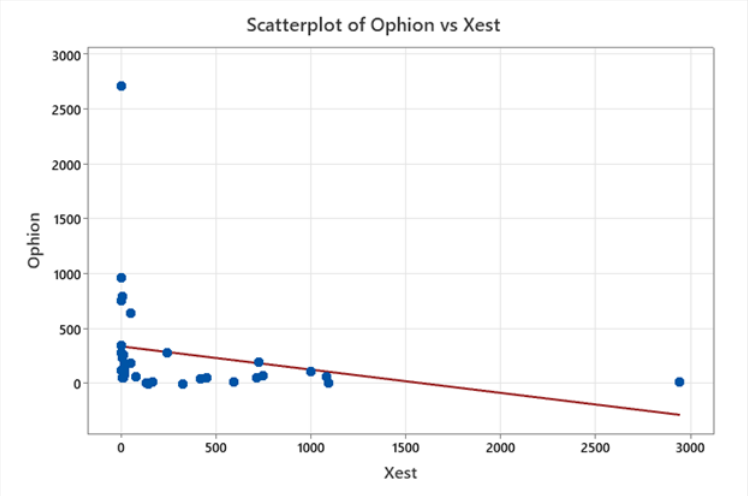

Figure 12: Numerical simulation of the stability of the (0,0) fixed point.

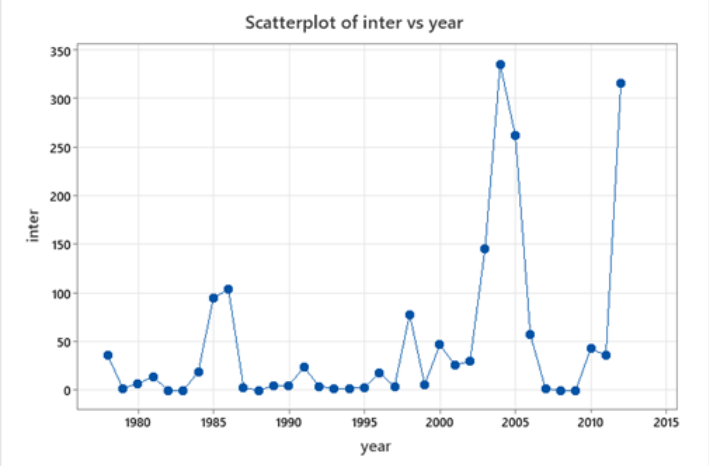

Figure 13: Interactions of Ophion and Xest with respect to years.

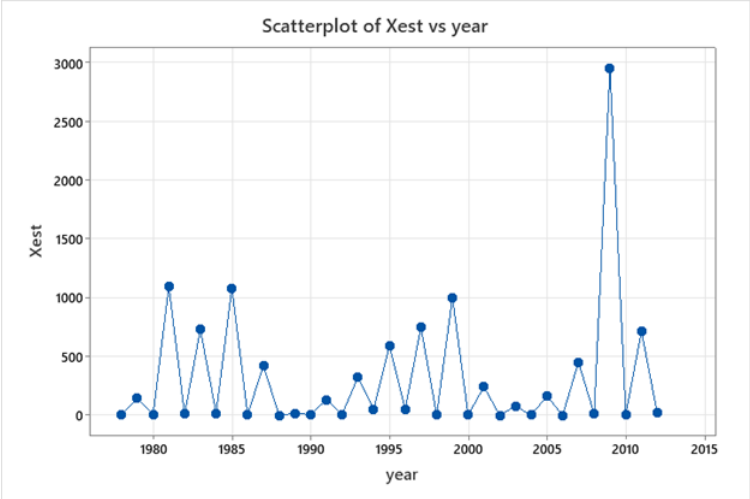

Figure 14: Time series of Xest.

References

[1] Joel Alba-Pérez and Jorge E Macías-Díaz. Analysis of structure-preserving discrete models for predator-prey systems with anomalous diffusion. *Mathematics*, 7(12):1172, 2019.

[2] John R Beddington. Mutual interference between parasites or predators and its effect on searching efficiency. *The Journal of Animal Ecology*, pages 331–340, 1975.

[3] Saber N Elaydi. *Discrete chaos: with applications in science and engineering*. Chapman and Hall/CRC, 2007.

[4] Edward W Evans. Dispersal in host–parasitoid interactions: Crop colonization by pests and specialist enemies. *Insects*, 9(4):134, 2018.

[5] James R Hepler, Kacie Athey, David Enicks, Paul K Abram, Tara D Gariepy, Elijah J Talamas, and Elizabeth Beers. Hidden host mortality from an introduced parasitoid: Conventional and molecular evaluation of non-target risk. *Insects*, 11(11):822, 2020.

[6] SOPHIA R-J Jang and Jui-Ling Yu. A discrete-time host-parasitoid model. In *Proceedings of the Conference on Differential and Difference Equations and Applications. Hindawi Publishing Corporation*, pages 451–455, 2006.

[7] Abdul Qadeer Khan and Muhammad Naeem Qureshi. Dynamics of a modified nicholson-bailey host-parasitoid model. *Advances in Difference Equations*, 2015(1):1–15, 2015.

[8] Burcin Kulahcioglu and Unal Ufuktepe. A density dependent host-parasitoid model with allee and refuge effects. In *Computational Science and Its Applications–ICCSA*

2016: 16th International Conference, Beijing, China, July 4-7, 2016, Proceedings, Part III 16, pages 228–239. Springer, 2016.

[9] Xiaorong Ma, Qamar Din, Muhammad Rafaqat, Nasir Javaid, and Yongliang Feng. A density-dependent host-parasitoid model with stability, bifurcation and chaos control. *Mathematics*, 8(4):536, 2020.

[10] RM May, MP Hassell, RM Anderson, and DW Tonkyn. Density dependence in host-parasitoid models. *The Journal of Animal Ecology*, pages 855–865, 1981.

[11] Marko Mutanen, Otso Ovaskainen, Gergely Várkonyi, Juhani Itämies, Sean WJ Prosser, Paul DN Hebert, and Ilkka Hanski. Dynamics of a host–parasitoid interaction clarified by modelling and dna sequencing. *Ecology Letters*, 23(5):851–859, 2020.

[12] Alexander J Nicholson and Victor A Bailey. The balance of animal populations.—part i. In *Proceedings of the zoological society of London*, volume 105, pages 551–598. Wiley Online Library, 1935.

[13] Ainara Peñalver-Cruz, Bruno Jaloux, and Blas Lavandero. The host-plant origin affects the morphological traits and the reproductive behavior of the aphid parasitoid aphelinus mali. *Agronomy*, 12(1):101, 2022.

[14] Serge Quilici and Pascal Rousse. Location of host and host habitat by fruit fly parasitoids. *Insects*, 3(4):1220–1235, 2012.

[15] M Rost, G Várkonyi, and I Hanski. Patterns of 2-year population cycles in spatially extended host–parasitoid systems. *Theoretical Population Biology*, 59(3):223–233, 2001.

[16] Bellie Sivakumar and Bhadran Deepthi. Complexity of covid-19 dynamics. *Entropy*, 24(1):50, 2022.

[17] Agus Suryanto, Isnani Darti, Hasan S. Panigoro, and Adem Kilicman. A fractional-order predator–prey model with ratio-dependent functional response and linear harvesting. *Mathematics*, 7(11):1100, 2019.

[18] Unal Ufuktepe and Sinan Kapcak. Applications of discrete dynamical systems with mathematica. *RIMS Kyoto Proceedings*, 1909:207–216, 2014.

[19] Saskya Van Nouhuys, Suvi Niemikapee, and Ilkka Hanski. Variation in a host–parasitoid interaction across independent populations. *Insects*, 3(4):1236–1256, 2012.

[20] Gergely Várkonyi, Ilkka Hanski, Martin Rost, and Juhani Itämies. Host-parasitoid dynamics in periodic boreal moths. *Oikos*, 98(3):421–430, 2002.

[21] Sandra Vaz and Delfim FM Torres. A discrete-time compartmental epidemiological model for covid-19 with a case study for portugal. *Axioms*, 10(4):314, 2021.

[22] Jianming Zhang, Lijun Zhang, and Yuzhen Bai. Stability and bifurcation analysis on a predator–prey system with the weak allee effect. *Mathematics*, 7(5):432, 2019.